Microwave Review
December 2024, Vol. 30, No. 2, pp. 71-81
DOI: 10.18485/mtts_mr.2024.30.2.9

Efficiency Enhanced Sneezewort Plant Inspired Antenna for mm-wave Applications

Tapan Nahar[1], Sanyog Rawat[2], Pallav Rawal[3], Vishal Das[4]

Abstract – **Stable radiation performance across a broad bandwidth, as well as high efficiency and gain antenna design, are essential criteria of mm-wave communication so that efficient low loss high speed low latency information transmission is possible, and path losses due to environmental absorptions may be avoided. The efficiency of conventional antenna design structures may be boosted by applying numerous strategies, but with the loss of structural planarity, cost effectiveness, and simplicity of manufacturing. A five-element sneezewort plant-inspired mm-wave antenna is presented, which employs the Fibonacci pattern and golden ratio in the width of branches and number of elements at each step. The proposed antenna operates between 28-62 GHz and 64-160 GHz, with radiation efficiency and total efficiency of 98.4% and 98.17%, respectively. It was made on a roggers RT duroid substrate with a thickness of 0.254 mm and has a flat geometry and may be suitable for various mm-wave applications. At the end, scaled down versions of antenna are presented which is fabricated and performance is measured.**

Keywords – **nature inspired antenna, sneezewort plant inspired antenna, mm-wave antenna, V-band antenna, M-band antenna, W-band antenna**

I. INTRODUCTION

Mm-Wave frequencies offer significant promise for ultra-high speed, low latency communication due to the availability of massive bandwidth. Although this band has advantages like a higher channel capacity and a small antenna size, it also has significant drawbacks like a small communication range, a high path loss, and environmental attenuation [1]. Due to their small size and large bandwidth, mm-wave antennas have unstable gain and efficiency[2]. Efficiency may be boosted by using methods to lessen conductor loss, dielectric loss, surface wave loss, and other losses [3]. Numerous techniques, such as a small loss substrate [4], electromagnetic band gap structure [5], defective ground structures [6], meta-material based structures [7], substrate integrated waveguide based feeding [8], removing a portion of the substrate[3], high dense dielectric antenna [9], multi-layer patch, etc., can be used to increase efficiency[3]. Obtaining consistent efficiency while maintaining broad bandwidth, flat shape, easy manufacture, and cheap cost are significant challenges. A multi-layered construction exhibited alignment issues, complicated production, and higher fabrication costs. The following problems may be resolved using architecture that are inspired by nature.

Designers of antennas are often inspired by natural structures since they exhibit effective radiation performance when compared to traditional antenna designs. Due to their architecture or orientation, natural trees and plants effectively collect electromagnetic energy from the sun. Numerous antenna designs inspired by nature have been proposed by researchers. An antenna that was inspired by sunflowers has been demonstrated [10]. The proposed antenna employs a Fibonacci pattern in a sunflower and is positioned at the seed. The suggested antenna has a frequency range of 12 to 17.4 GHz and a maximum gain of 6.2 dB within a 20x20x1.59 mm3 dimension. The spiral-shaped gap between succeeding antenna components acts as a leaking cavity, representing a rise in incoming wave magnitude caused by the presence of the seed cavity[11]. The efficiency of the proposed antenna ranges from 60 to 65%. A golden spiral-based Snail's shell-inspired antenna is shown in [12] and it employs radiuses that follow the Fibonacci sequence. To achieve broad bandwidth and merge several modes together, a partial ground structure with two semi-ring-shaped slots is employed. The proposed antenna has a maximum radiation efficiency of 90% and operates between 1 and 35 GHz. But a significant drawback is the gain's fluctuation. A gain of 5.3 dB maximum is attained. [13] Presents a microstrip antenna in the form of a flower with four leaves and diagonal symmetry. All of the modes are coupled within the same bandwidth using a partial ground plane. The proposed antenna has a maximum gain of 3 to 4 dB and 49% bandwidth at 1.975 GHz. A flower shaped MIMO antenna is presented in [14] with T like ground plane. Proposed antenna provides 85-93% efficiency. With gain in the range of 2.5 to 5.35 dB and operating at 4.3-15.63 GHz. [15] presents a flower-shaped antenna with a rectangular ring resonator for 1.1 THz applications. The proposed antenna has a gain of 12.78 dB and a bandwidth of 710 GHz. For THz applications, eight Patel flower-shaped antenna are given in [16]. With a frequency range of 6.04 THz (0.56–6.60 THz), the proposed antenna offers 12.5 dB gain. For mmwave applications, five circular Patel-based MIMO antennas are given in [17].At 28 GHz, the suggested antenna offers gain of 8 dB and 95% efficiency. In [18], a flower-shaped antenna with a gain of 6.57 dB and a bandwidth of 5.96 THz is shown.

In [19], a multiband tree-shaped antenna with resonances at 9.3 GHz, 10.07 GHz, 11.76 GHz, and 13.16 GHz with a gain of 6 to 10.15 dB is reported. The suggested antenna offers almost constant gain across a range of frequencies. Slitted three leaf element antenna in the form of a flower is shown in [20]. The proposed antenna has dual band properties and

Article history: Received May 30, 2023; Accepted October 03, 2024.

[1]Tapan Nahar is with Department of Information and communication Technology, Marwadi University, Rajkot, India,
[2]Sanyog Rawat is with Department of Electronics and Communication Engineering at Central University of Rajasthan, India, E-mail: sanyog.rawat@curaj.ac.in,
[3]Pallav Rawal is with Deptt. of ECE, SKIT, Jaipur,
[4]Vishal Das is with Deptt. of ECE, Manipal University Jaipur.

5.2 GHz radiation efficiency of 96%. Gain varies greatly between lower and higher resonant frequencies. [21] presents a maple-leaf-shaped antenna for use in THz optical applications. The proposed antenna offers gain in the range of 8.02 to 11.4 dB, 400 GHz bandwidth, and 60% efficiency at 193.5/229/352.9/393 THz. [22] presents a 21 branch antenna with slotted ground that was inspired by Achillea Ptarmica. The proposed antenna has a maximum gain of 5 dB and a maximum radiation efficiency of 70%. It works between 8.2 and 16.5 GHz. Radiation efficiency exceeding 90% and steady gain have only been seen in very few studies. Although a nature-inspired antenna may be used to increase efficiency and improve radiation characteristics, this possibility has not been sufficiently investigated. A major research gap is the simultaneous achievement of wide bandwidth, stable efficiency, and gain. At mm-wave frequencies, very little research has been done on the nature-inspired antenna. Comparison of the reported and suggested antennas that were inspired by nature is presented in Table 1.

This article describes a sneezewort plant-inspired antenna with efficiency above 98%, wide bandwidth, and consistent gain at mm-wave frequencies from 28 GHz to 160 GHz, which may be utilised for diverse V band, W band, M band, and upcoming 6G wireless applications. The breadth of the branches and the number of elements in the design follow the Fibonacci pattern and the golden ratio. With regard to antenna performance parameters, comparisons of two element, three element, and five element antennas are conducted.

TABLE 1
COMPARISON OF THE PERFORMANCES OF REPORTED NATURE INSPIRED ANTENNAS AND PROPOSED ANTENNAS

Structure	Operating frequency GHz	Radiation Efficiency (%)	Gain (dB)
Sunflower[23]	12-17.44	65%	6
Slits three leaf element flower shaped antenna [20]	2.1 and 5.2	52.5%/96%	−2.1/ 2.9
Golden spiral based Snail's shell inspired antenna [12]	1-35	90%	5.3
Flower shaped MIMO antenna[14]	4.3-15.63	85-93%	2.5-5.35
Maple-Leaf Shaped antenna[21]	45-450	60 %	8.02-11.4
Five circular patel based MIMO antenna [17]	28-30GHz	95%	8
Achillea Ptarmica inspired 21 branch antenna[22]	8.2 to 16.5	70%	4.616
This work 2-element sneezewort plant antenna	32-60	97.05	6.050
This work 3-element sneezewort plant antenna	32.5-63	98.9	6.563
This work 5-element sneezewort plant antenna	28-62 GHz 64-160	98.4	

Paper is divided into seven sections. The first section discusses mm-wave antenna performance requirements, literature reviews, and research gaps. The second part discusses the design of the antenna and the computation of the design parameters for the sneezewort plant-inspired antenna. The simulation results for antenna are covered in the third part. Parametric analysis is presented in section fourth. In the fifth part, performance comparisons with various antennas are covered. Scaled down version of antenna is presented in Section VI. The seventh portion includes the conclusion.

II. ANTENNA DESIGN

Studies on mm-Wave and antenna design are motivated by natural plant and tree architectures. Natural vegetation organises its leaves and stems to maximise the amount of solar rays (EM waves) that may be used for photosynthesis. Antenna designs influenced by nature have shown to be effective. The golden ratio and natural Fibonacci patterns were studied in order to construct the antenna model that is provided in the article [22]. The golden ratio may be observed in nature, as well as in many urns, modern buildings, playing cards, and works of art by Leonardo da Vinci. The Fibonacci sequence is the pattern that was utilised to construct the branches. The common name for one of these plants is sneezewort (Achillea Ptamrica). Fig. 1 (a), (b), and (c), respectively, show two element, three element, and five element sneezewort plant inspired antenna structures.

The number of branches at stage 3 equals the total of the two stages before it, or 1 + 2 = 3, if the initial number of branches at stages 1 and 2 is 1 and 2, respectively. The arrangement of branches in the structure that was inspired by the sneezewort plant is shown in Fig. 1(c). The Fibonacci sequence may be created using the following equation (1).

$$Fn = Fn\text{-}1 + Fn\text{-}2;\ n = 2, 3, 4. \quad (1)$$

Table 2 shows how the number of branches in the antenna that was inspired by the sneezewort plant uses the Fibonacci pattern. At each level, the golden ratio may be used to calculate the breadth of new arms. If the initial width is W1, and the new arm widths are W1.1 and W1.2, W1.2 can be obtained by deducting W1.1 from W1 and W1.1 can be determined by dividing W1 by the golden ratio (1.618).

$$W1.1 = W1 / 1.618;\ W1.2 = W1 - W1.1. \quad (2)$$

TABLE 2
FIBONACCI PATTERN IN THE NO. OF ELEMENTS IN SNEEZEWORT PLANT STRUCTURE

No. elements at first stage (F_1)	1
No. elements at second stage (F_2)	2
No. elements at third stage ($F_{3=} F_1 + F_2$)	3
No. elements at forth stage ($F_{4=} F_2 + F_3$)	5

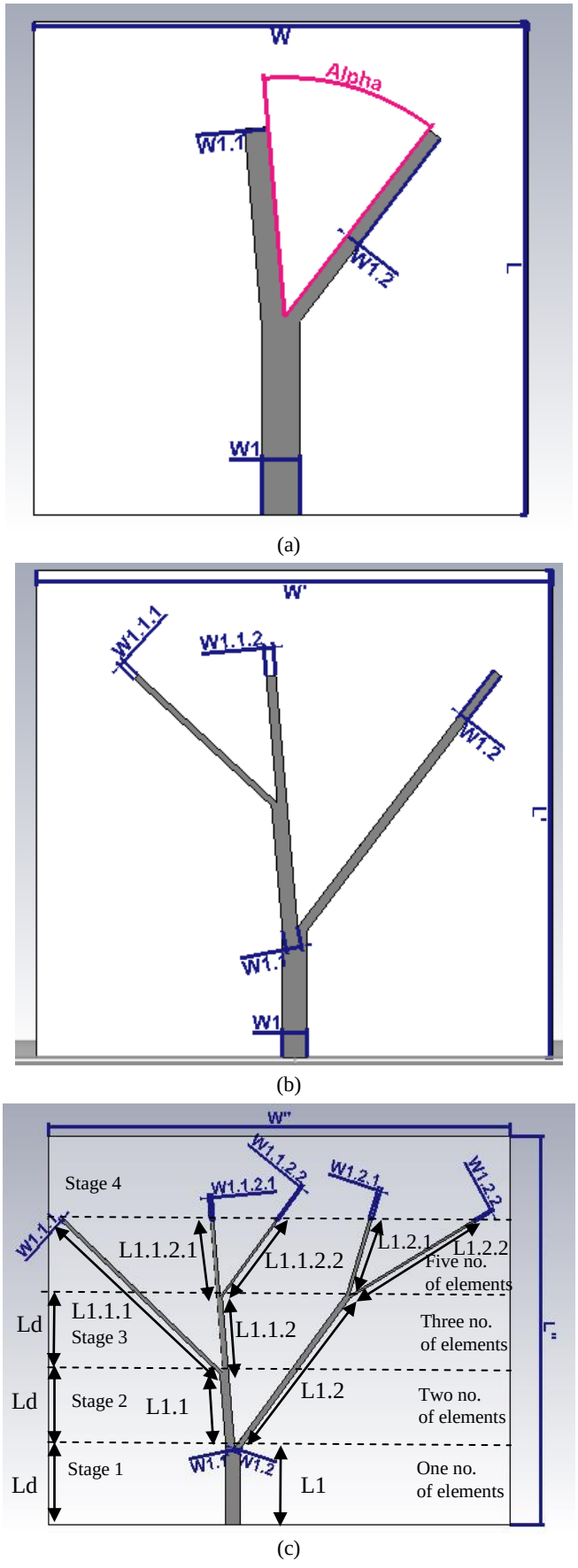

Fig. 1. Proposed sneezewort plant inspired antenna geometry: (a) Two Stage, (b) Three Stage, (c) Four Stage

The method is the same for succeeding branches. The new branch's angle follows the golden angle of 137.5 degrees. (180-137.5) degrees is the angle (alpha) between the new branches. All the design parameters for the suggested antennas are shown in Table 3 and dimensions are in mm. On a Roggers RT duroid substrate with a dielectric constant of 2.2, a loss tangent of 0.0009, and a thickness (h) of 0.254 mm, all of the antennas were constructed. Thickness of metallic layer (t) used for patch and ground is 0.035 mm. Lg_1, Lg_3, and Lg_5 are the ground plane length of two stage antenna, three stage and four stage antenna respectively. Other parameters are indicated in Fig.1.

TABLE 3
DESIGN PARAMETERS OF PROPOSED ANTENNAS

W1	L1	W1.1	L1.1	W1.2	L1.2
0.78	3.916	0.48	3.87	0.3	9.86
L1.1.2	W1.1.2	L1.1.1	W1.1.1	L1.1.2.1	W1.1.2.1
3.92	0.29	11.52	0.19	3.92	0.18
L1.1.2.2	W1.1.2.2	L1.2.1	W1.2.1	L1.2.2	W1.2.2
4.85	0.11	4	0.18	7.7	0.11
Ld	L	W	L’	W’	L’’
4	10	10	15	16	20
W’’	Lg_1	Lg_3	Lg_5	h	t
25	6.5	10	9.95	0.254	0.035

III. SIMULATION RESULTS

Fig. 2 displays the reflection coefficient vs frequency plot of two, three, and five element antennas that were inspired by sneezewort plants. It can be shown that the two-element, two-stage sneezewort construction delivers 53.43% bandwidth at 52.4 GHz and resonates from 32 GHz to 60 GHz with reflections less than 10 dB. At 52.4 GHz, the minimum S11 is -37 dB and average S11 is -14.67 dB over operating band. Operating band is enhanced by 3.5 GHz when a three stage or three element structure is utilised in contrast to a two element configuration. The resonance frequency is moved from 52.4 to 60 GHz. The antenna's % bandwidth is reduced from 53.43% to 50.83%, and its minimum reflection coefficient improves to -43 dB at 60 GHz. Average reflection coefficient is -14.29 dB which is almost same or slightly less than average reflection coefficient of two element structure. An extra band of resonance is created when a four stage, five element sneezewort structure is utilised. Four-stage structures give bandwidth of 59.6% and 65.30% at 57.04 GHz and 147 GHz, respectively, while operating between 28 and 62 GHz and 64 and 160 GHz. At 57.04 GHz and 147 GHz, the minimum reflection coefficients are approximately -42 dB and -43 dB, respectively, indicating good matching. Average reflection coefficient is -17.56 dB and -15.02 dB in first band and second band. This shows the improvement of impedance matching at whole operating band in comparison to two element and three element structure. When using partial ground plane and multiple elements, it is possible to obtain a wide bandwidth by integrating multiple bands below -10 dB S11. The feed and patch impedances are properly matched as seen by the minimum reflection coefficients and average

reflection coefficients. Electromagnetic simulation tool Computer simulation technology microwave studio (CST Microwave Studio) is used for simulation. The operating range, bandwidth, and reflection coefficients for the single-stage, double-stage, and three-stage sneezewort plant-inspired structures are compared in Table 4.

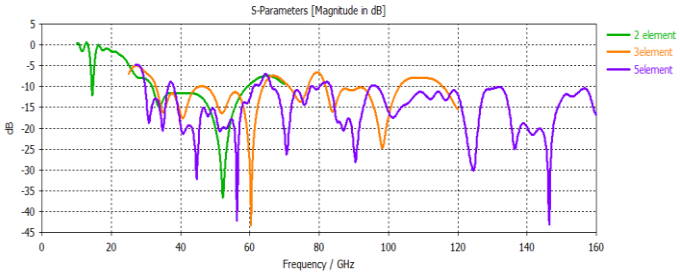

Fig. 2. Reflection coefficient (S11) versus frequency plot

TABLE 4
COMPARISONS OF OPERATING RANGE BANDWIDTH AND S11

S.No.	No. of Element	Operating Range (Bandwidth %)	Min. S11 (dB)	Average S11 (dB)
1	2	32-60 GHz (53.43%)	-37 dB at 52.4 GHz	-14.67
2	3	32.5-63 GHz (50.83%)	-43 dB at 60 GHz	-14.29
3	5	28-62 GHz (59.6%) 64-160 GHz (68.57%)	-42 dB at 57.04GHz -43 at 147 GHz	-17.56 -15.02

Fig. 3 (a), (b), and (c), respectively, show the surface current density of the two-element, three-element, and five-element sneezewort plant structures. The most current is focused at the edges and in the final stage of the sneezewort-based construction at all phases, which suggests that the structure has effective radiating capabilities. Efficiency and performance improved as the number of components rose.

By examining the radiation patterns, the far field performance of the suggested antennas is calculated. Consolidated radiation patterns for all antennas are shown in Fig. 4(a) and (b) at Phi=0 degree and Phi=90 degree, respectively. Gain increases and beamwidth narrows as the number of elements increases, indicating an improvement in the antenna's radiating capabilities and directionality. Due to the many elements and radiations from the feeding structure, two element structures offer the smallest number of lobes, while five element structures produce the highest number of lobes. It is evident from the three-dimensional plots for 2 element, 3 element, and 5 element structures shown in Fig. 5(a), (b), and (c). At 52.2 GHz, the maximum gain of two-stage, three-stage, and five-stage structures is 4.616 dB, followed by 6.05 dB, and 6.56 dB. Beamwidths at half power are 75.3 degrees, 69.6 degrees, and 20.8 degrees. The overall efficiencies for a two-element, three-element, and five-element structure are 96.08%, 97.04%, and 98.17%, respectively. It can be shown that efficiency increases as the number of branches increases, indicating a decrease in overall losses. Table 5 compares gain, radiation efficiency and total efficiency of all the structures at 52.2 GHz.

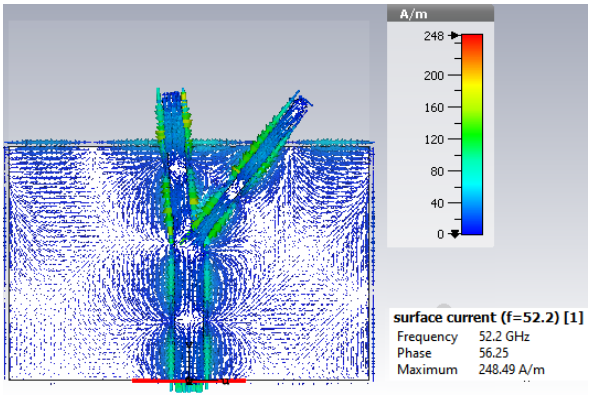

(a)

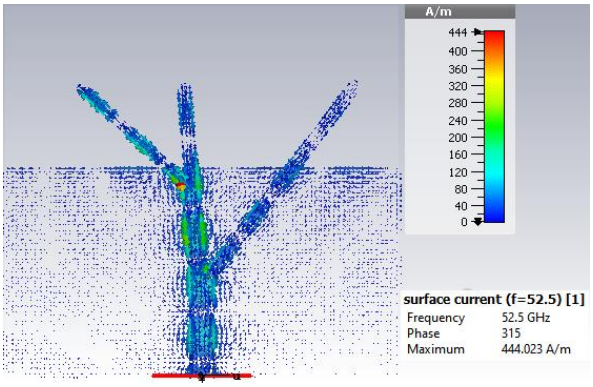

(b)

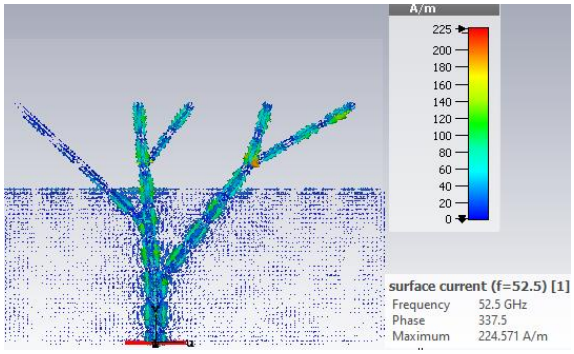

(c)

Fig. 3. Suface current distribution: (a) Two element, (b) Three element, (c) Five element

TABLE 5
COMPARISONS OF GAIN, HPBW, RADIATION EFFICIENCY AND TOTAL EFFICIENCY AT 52.2 GHZ

No. of Element	Gain (dB)	HPBW (Phi=0)	Radiation Efficiency %	Total Efficiency %
2	4.616	75.3	97.05	96.08
3	6.050	69.6	98.9	97.04
5	6.563	20.8	98.4	98.17

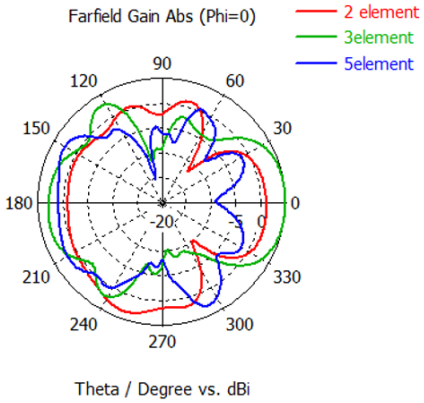

(a)

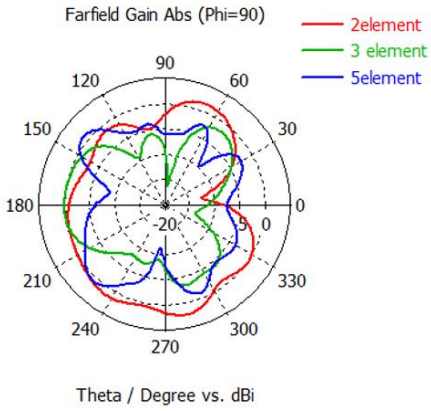

(b)

Fig. 4. Consolidated radiation pattern at 52.2 GHz:
(a) at Phi=0, (b) at Phi=90 deg

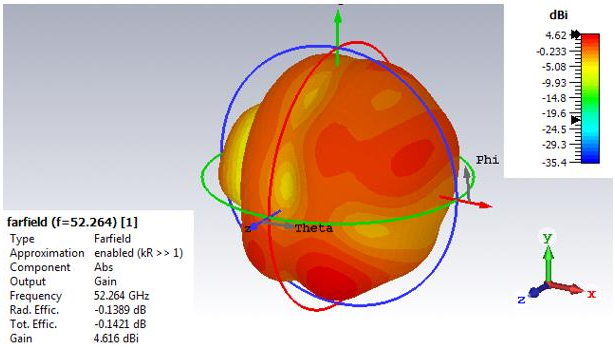

(a)

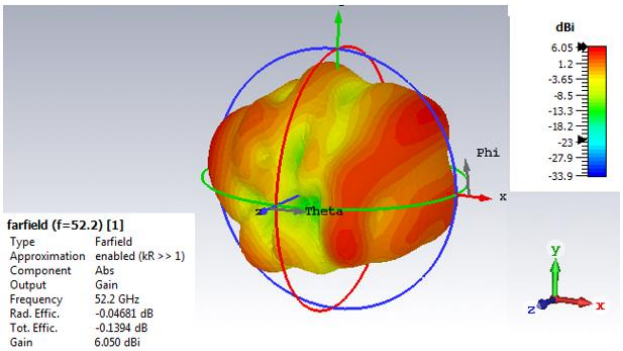

(b)

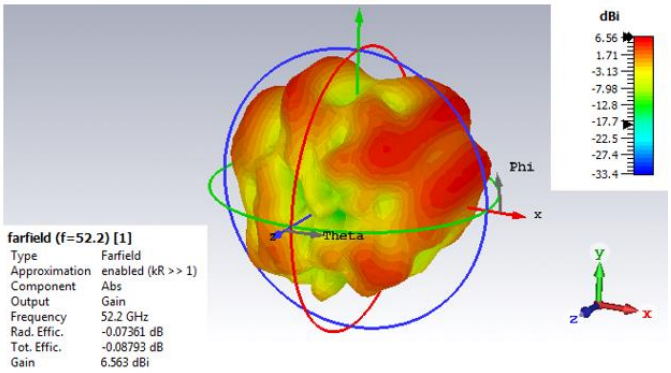

(c)

Fig. 5. Three dimensional radiation pattern at 52.2 GHz:
(a) Two element, (b) Three element, (c) Five element

Fig. 6 displays the gain versus frequency curve for each structure. Gain is raised and reaches its maximum at higher frequencies, as can be shown. The gain response is displayed between the individual structure's minimum and highest operating frequencies. At all operating frequencies, a five element structure has a maximum gain of about 12 dB and greater. When seen separately, gain variations for each operating band are around 3 dB, but when the entire band is tallied, the discrepancies between the first and second operating bands are somewhat bigger.

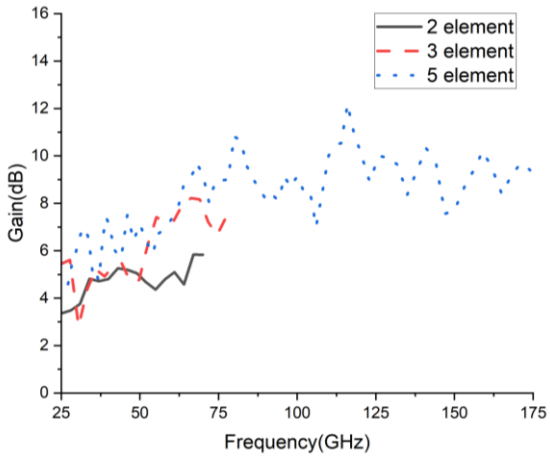

Fig. 6 Gain (dB) versus frequency plot

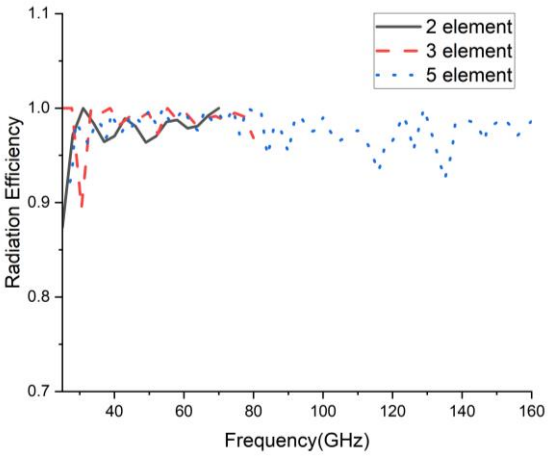

Fig. 7. Radiation efficiency versus frequency plot

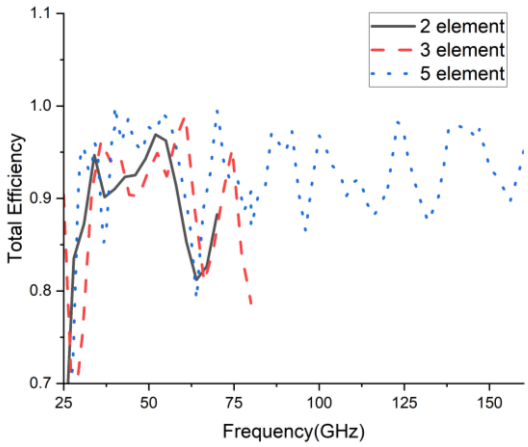

Fig. 8. Total efficiency versus frequency plot

Fig. 7 compares the radiation efficiency vs. frequency plots of all structures. The key benefits of nature-inspired structures are minimal losses and effective radiation capabilities, as shown by the observation that radiation efficiency is above 97% for all structures over the operational band. According to Fig. 8, the highest overall efficiency for all structures is likewise higher than 95%. Total efficiency is greater than 80% for the operating band as a whole. The greatest efficiency of a construction is five elements.

IV. Parametric Analysis

A. Effect of stage length on performance of antenna:

The length of the branching elements is structured, as seen in Fig. 1, so that the vertical length (Ld) of each stage stays constant. The S11 versus frequency plot is observed when Ld is changed from 2 mm to 5 mm, and it is displayed in Fig. 9. It can be seen that resonance is more efficient at lower frequencies and that antenna size increases as length Ld increases. The feed line should be half wavelength long for both narrow band and complete ground plane operation. Because the operating wavelength has a wide range, length can be lowered and extended up to a specified length for wide band operation and partial ground plane design. Partial ground plane tuning allows for the tuning of many modes across a broad range.

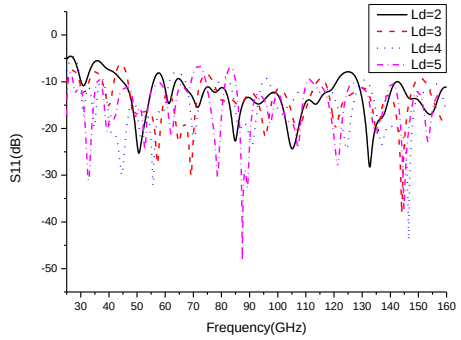

Fig. 9. S11 versus frequency plot for various stage length (Ld)

Plot of gain versus frequency for different stage lengths Ld is shown in Fig.10. Gain reaches its greatest at 102 GHz for a 3 mm of Ld, but it exhibits distinct trends at other frequencies. The physical size of the antenna is big at Ld=5 mm and Ld=4 mm. In general, gain can be enhanced by increasing antenna area, but efficiency also plays a role.

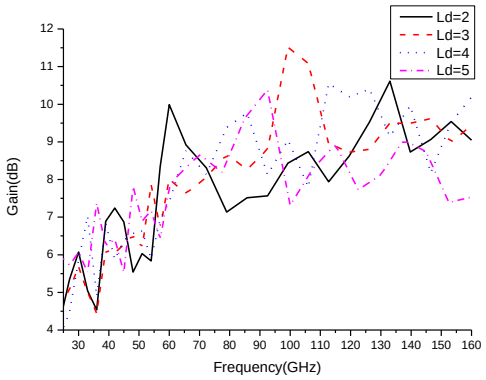

Fig. 10. Gain versus frequency plot for various stage length (Ld)

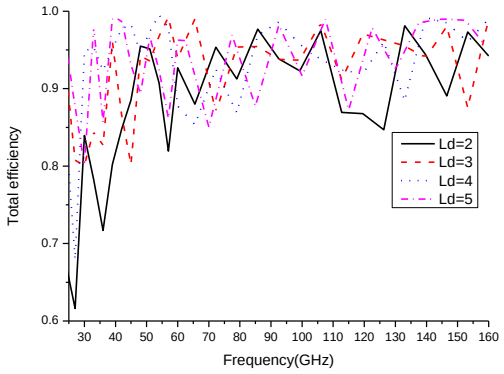

Fig. 11. Total efficiency versus frequency plot for various stage length (Ld)

Fig. 11 displays the total efficiency versus frequency plot for different stage lengths. For the majority of frequencies, the stage lengths of 4 mm and 5 mm have the highest efficiency. Efficiency is lowest across the majority of the band at Ld=2 mm.

B. Effect of feed line width on performance of antenna:

Fig. 12 shows the reflection coefficient vs frequency plot for feed line width W1 of 2 mm, 3.05 mm, and 0.78 mm. For roggors RT duroid substrate with full ground and substrate thickness of 0.254 mm, the 50 ohm line has a width of 0.78 mm. It can be seen that the S11 is less than -20 dB at several frequency bands with an initial width of 0.78 mm. In the three frequency band, S11 is less than -20 dB for W1 of 3.05 and W1 of 2 mm. The total bandwidth for each of these W1 is nearly the same.

Fig. 13 shows the gain versus frequency curve for each of the three element widths. When W1 of 0.78 mm is utilized, gain varies by 4-5 dB over the working band. Although using W1 of 3.05 mm and 2 mm yields maximum gain at specific frequencies.

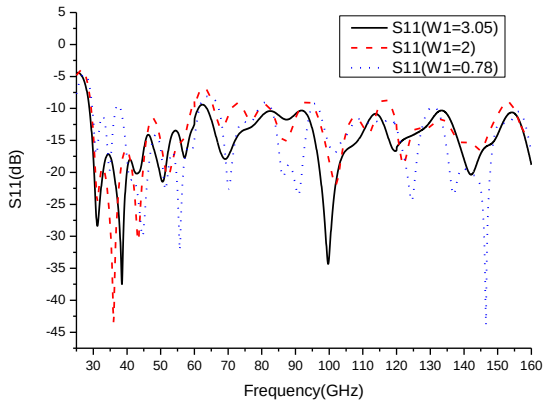

Fig. 12. S11 versus frequency plot for various initial width W1

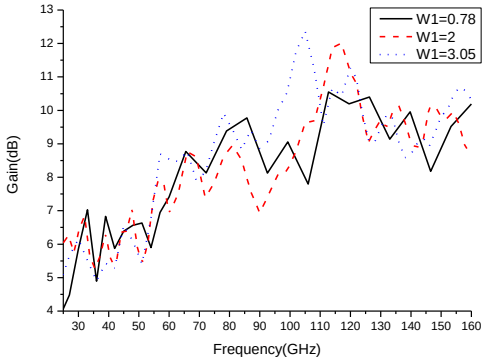

Fig. 13. Gain versus frequency plot for various initial width W1

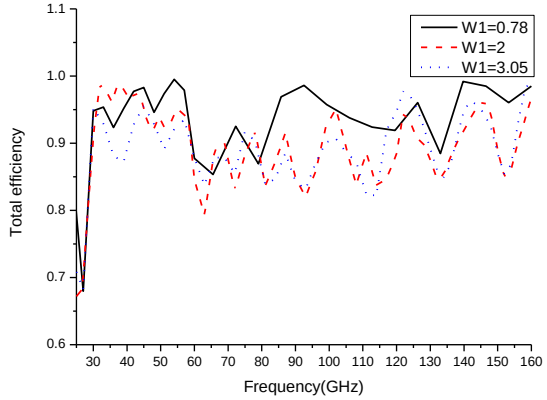

Fig. 14. Total efficiency versus frequency plot for various initial width W1

Fig. 14 shows the total efficiency vs frequency curve for different W1. When W1 is 0.78 mm, stable efficiency between 0.85 and 0.99 is attained. Over the working band, efficiency changes are significant for W1 values of 2 mm and 3.05 mm.

V. Performance Comparisons with Reported Antennas

Table 6 contrasts the proposed antenna's performance with those of mm-wave antennas that have already been described. It should be noted that the suggested antenna offers strong gain, wide bandwidth, and the maximum efficiency.

TABLE 6
PERFORMANCE COMPARISON OF PROPOSED ANTENNA WITH REPORTED 60 GHZ ANTENNAS

Work	Antenna Type	Operating Range (GHz)	Impedance Bandwidth (%)	Radiation Efficiency and Total efficiency (%)	Peak Gain (dBi)
This work	2 element sneezewort plant inspired antenna	32-60	53.43	97.05 and 96.08	4.616
This work	3 element sneezewort plant inspired antenna	32.5-63	50.83	98.9 and 97.04	6.050
This work	5 element sneezewort plant inspired antenna	28-62 and 64-160	59.6 68.57	98.4 and 98.17	6.563
[24]	Electromagnetically coupled Semi-circular microstrip antenna	58.4-100	70.83	88.1 and 85.3	5.23
[25]	Parasitic coupled rectangular antenna	42-68.1	47	95	4
[26]	Circularly polarized	50-70	26	90	7
[27]	Patch antenna with recessed ground	58.2-65	11.33	87.44	6.94
[28]	Superstrate Antenna	58.7-62.7	6.8	76	14.6
[29]	CPW fed post supported patch antenna	58.7-64.5	14.5	94	9.9
[30]	V shaped 3D dipole	57-66	14.3	77.8	5.45
[31]	Charge slot antennas with diffused engineered line	-	4.76	-	5.48
[32]	Photonic band gap antenna	52-64	20.53	75.53	7.9
[33]	Circular dish microstrip antenna with ring slot	59-62.5	5.7	95	3.9
[34]	Metasurface antenna	53.3-67	22.83	-	5.5

VI. SCALED DOWN VERSION OF ANTENNA

In India, antenna measuring facilities are developed or only accessible up to the 18 GHz frequency range. There are few locations where measurements at higher frequencies are possible, but it is not accessable to authors. A low-cost, scaled-down prototype of the antenna is simulated, constructed, and measured in order to demonstrate the validity of the suggested antenna. The table displays the design parameters for a five-element antenna inspired by the sneezewort plant. Scaled version is fabricated on FR4 substrate having height of 1.6 mm, dielectric constant of 4.3 and, loss tangent of 0.025. Fabricated antenna has been shown in Fig. 15.

TABLE 7
DESIGN PARAMETERS OF SCALED DOWN VERSION OF PROPOSED ANTENNAS

W1	L1	W1.1	L1.1	W1.2	L1.2
3.05	21.93	1.91	21.86	1.14	55.81
L1.1.2	W1.1.2	L1.1.1	W1.1.1	L1.1.2.1	W1.1.2.1
21.9	0.72	65.84	1.19	21.87	0.44
L1.1.2.2	W1.1.2.2	L1.2.1	W1.2.1	L1.2.2	W1.2.2
27.96	0.27	21.93	0.71	41.95	0.43
Ld	L''	W''	Lg_5	h	t
21.93	100	190	77	1.6	0.035

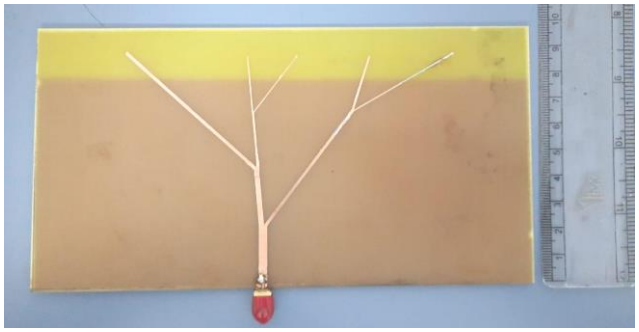

Fig. 15. Scaled down version of fabricated antenna

Fig. 16 displays the S11 vs frequency curve of the antenna's reduced size. The performance of simulated and fabricated antennas is nearly same, yet there are minor variations in the reflection coefficient. With the exception of some frequencies from 3.9 GHz to 4.36 GHz, where S11 is -10 dB to -5 dB, the simulated antenna is tuned from 3 GHz to 18 GHz. The frequency range of the manufactured antenna is 3 GHz–18 GHz. Over the entire operational range, S11 is below -10 dB. The smallest slots in the ground plane and manufacturing flaws cause differences in the performance of the simulated and actual antennas.

Fig. 17(a), (b), (c), and (d) shows the measured and simulated radiation pattern at Phi=0 and Phi=90 deg. at 3.74 GHz, 5.92 GHz, 11.82 GHz, and 15.685 GHz, respectively. The performances of various parameters of constructed and simulated antennas are compared in Table 8. Each antenna's bandwidth is the same at -6 dB but somewhat varied at -10 dB because to flaws in the construction process. The manufactured antenna's gain is lower than that of the simulated antenna. However, patterns are quite similar. The observed gains are -0.74 dB, 3.12 dB, 2.5 dB, and -1.1 dB, while the highest gain of the simulated antenna at Phi=0 deg. is 0 dB, 5 dB, 3.6 dB, and 0.1 dB at 3.74 GHz, 5.92 GHz, 11.82 GHz, and 15.685 GHz. At 3.74 GHz, 5.92 GHz, 11.82 GHz, and 15.685 GHz, the simulated antenna gains at Phi=90 degree are 2.5 dB, 3.55 dB, -10 dB, and 2.7 dB, respectively, whereas the Measured gains are 2.34 dB, 3.32 dB, -7.5 dB, and 2.5 dB.

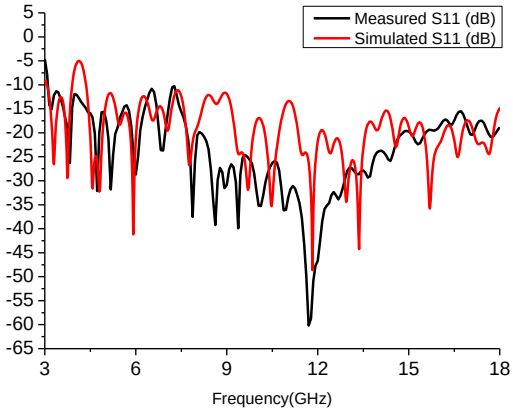

Fig. 16. S11 versus frequency curve of Scaled down version of fabricated antenna

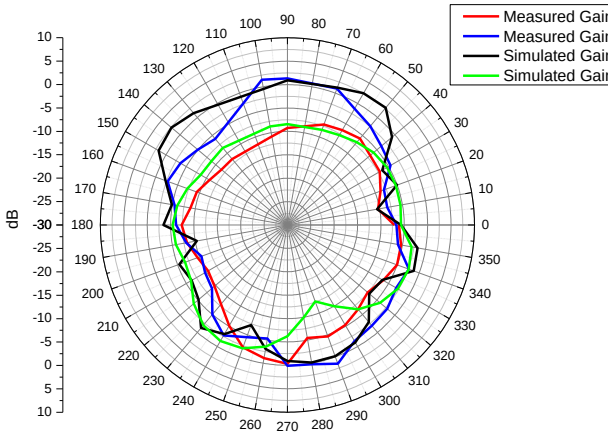

(a)

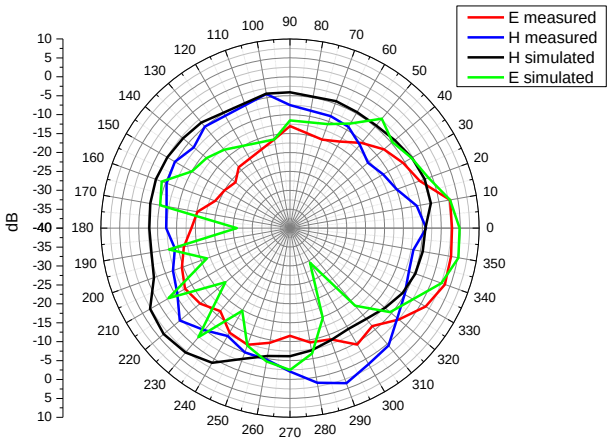

(b)

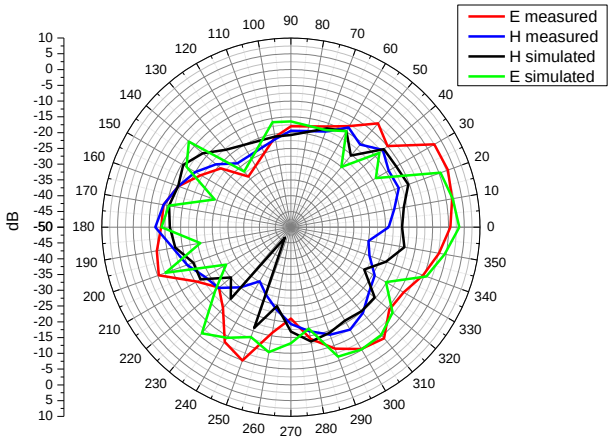

(c)

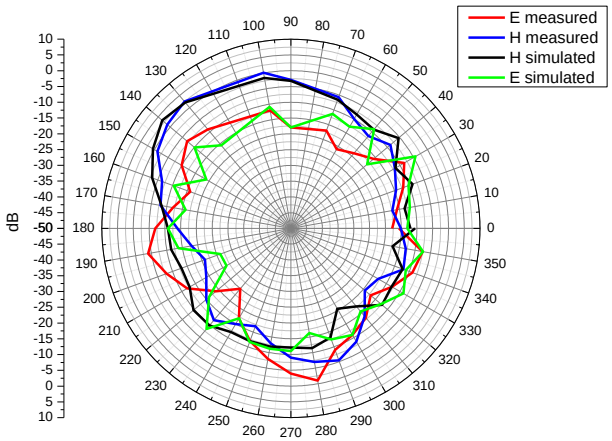

(d)

Fig. 17. Simulated and Measured Radiation Pattern at Phi=0 and Phi=90 degree of Scaled down version of fabricated antenna at: (a) 3.74 GHz, (b) 5.92 GHz, (c) 11.82 GHz, (d) 15.685 GHz

TABLE 8
PERFORMANCE COMPARISON OF SIMULATED AND FABRICATED SCALED DOWN ANTENNA

Parameters	Simulated Antenna	Fabricated Antenna
Frequency range where S11<-10 dB	3-3.9 GHz and 4.36-18 GHz	3-18 GHz
Impedance Bandwidth (%)	24.06% at 3.74 GHz 115.39% at 11.82 GHz	126.90% at 11.82 GHz
Maximum Gain (dB) at Phi=0	0 dB at 3.74 GHz 5 dB at 5.92 GHz 3.6 dB at 11.82 GHz 0.1 dB at 15.685 GHz	-0.74 dB at 3.74 GHz 3.12 dB at 5.92 GHz 2.5 dB at 11.82 GHz -1.1 dB at 15.685 GHz
Maximum Gain (dB) at Phi=90	2.5 dB at 3.74 GHz 3.55 dB at 5.92 GHz -10 dB at 11.82 GHz 2.7 dB at 15.685 GHz	2.34 dB at 3.74 GHz 3.32 dB at 5.92 GHz -7.5 dB at 11.82 GHz 2.5 dB at 15.685 GHz

Table 9 presents a performance comparison of the proposed antenna with a scaled down antenna that uses FR4 and Rogers. It is evident that an antenna based on rogers has an efficiency of above 95% and a strong gain as a result. This paper presents a scaled-down version of the FR4-based system that was previously described and manufactured.

TABLE 9
PERFORMANCE COMPARISON BETWEEN PROPOSED ANTENNA AND SCALED DOWN ANTENNA

Parameters	Proposed Antenna	Roggers based Scaled down Antenna	FR4 Scaled down Antenna
Size	20x16x0.254 mm^3	190x100x0.254 mm3	190x100x1.6 mm^3
Ground Plane Length	9.95 mm	79 mm	77 mm
Substrate Matarial	Roggers RT duroid (Dielectric constant of 2.2, a loss tangent of 0.0009)	Roggers RT duroid (Dielectric constant of 2.2, a loss tangent of 0.0009)	FR4 (Dielectric constant of 4.3 and, loss tangent of 0.025)
Frequency range where S11<-10 dB	28-62 GHz and 64-160 GHz	6.86-9.69 GHz 10.49-14.456 GHz 15.224-19.63 GHz	3-3.9 GHz and 4.36-18 GHz
Impedance Bandwidth (%)	59.6% at 57.04 GHz 68.57% at 147 GHz	34.19% at 8.275 GHz 34.28% at 12.47 GHz 25.28% at 17.4 GHz	24.06% at 3.74 GHz 115.39% at 11.82 GHz
Maximum Gain (dB)	6.563 dB	9.74 dB	5 dB
Radiation Efficiency (%)	97.05%	97%	61.859%

Roggers has a low loss tangent, while FR4 has a high loss tangent. When minimal cost is needed, FR4 is utilized at lower frequencies. While using Rogers results in an efficiency of 97%, the efficiency of FR4 is poor at 61.898% due to its large loss tangent. As a result, the FR4 antenna's gain is lower whereas the Rogers-based antenna's gain is higher. The FR4-based antenna's large bandwidth is caused by its thick substrate. Due to a partial ground plane, both the FR4 and the scaled-down Roggers antennas are created in the same area; otherwise, the FR4 size should be low and the Roggers based antenna's size will be high.

VII. CONCLUSION

The nature-inspired sneezewort plant-based antenna for mm-wave applications is presented in this study. A comparison of many characteristics, including efficiency, bandwidth, gain, beamwidth, and others, is offered along with performance analyses of 2 element, 3 element, and 5 element structures. All of the structures have flat geometry, which

facilitates ease of manufacture, and more than 97% radiation efficiency. The gain, bandwidth, and efficiency of the proposed antennas improve as the number of stages rises. Stages can be chosen based on the requirements of the application. The proposed antenna covers the major portion of the Ka band, V band, W band, and M band and finds use in a variety of mm-wave imaging applications, satellite radar, future communication systems, airport security screening, health status monitoring, and many other mm-wave imaging applications.

ACKNOWLEDGEMENT

We extend our thanks to the ECE Department of Manipal University Jaipur for giving us laboratory resources and simulation facilities. Heartfelt gratitude to Swami Keshvanand Institute of Technology, Management & Gramothan, Jaipur, for providing assistance with manufacturing. We are grateful to the ECE Department of Govt. Mahila Engineering College, Ajmer, for offering measuring facilities. Their contributions were critical to the successful completion of our research. We appreciate the collaborative help from these organizations.

REFERENCES

[1] D. S. Agarwal, "Concurrent 60/94 GHz SIR Based Planar Antenna for 5G/MM-Wave Imaging Applications," *Wirel. Pers. Commun.*, vol. 121, pp. 1–11, Dec. 2021, DOI: 10.1007/s11277-021-08691-x.

[2] M. H. Dahri, M. I. Abbasi, M. H. Jamaluddin, and M. R. Kamarudin, "A Review of High Gain and High Efficiency Reflectarrays for 5G Communications," *IEEE Access*, vol. 6, pp. 5973–5985, 2018, DOI: 10.1109/ACCESS.2017.2786862.

[3] T. Nahar and S. Rawat, "Efficiency enhancement techniques of microwave and millimeter-wave antennas for 5G communication: A survey," *Trans. Emerg. Telecommun. Technol.*, vol. n/a, no. n/a, p. e4530, DOI: https://doi.org/10.1002/ett.4530.

[4] K. P. R. Girish Kumar, *Broadband Microstrip Antenna*. Artech House, 2003.

[5] G. Saxena, P. Jain, and Y. K. Awasthi, "High diversity gain super-wideband single band-notch MIMO antenna for multiple wireless applications," *IET Microwaves, Antennas Propag.*, vol. 14, no. 1, pp. 109–119, 2020, DOI: https://doi.org/10.1049/iet-map.2019.0450.

[6] S. Zhu, H. Liu, P. Wen, Z. Chen, and H. Xu, "Vivaldi Antenna Array Using Defected Ground Structure for Edge Effect Restraint and Back Radiation Suppression," *IEEE Antennas Wirel. Propag. Lett.*, vol. 19, no. 1, pp. 84–88, 2020, DOI: 10.1109/LAWP.2019.2953912.

[7] S. Senthilkumar, U. Surendar, X. S. Christina, and J. William, "A Compact Phased Array Antenna for 5G MIMO Applications," *Wirel. Pers. Commun.*, no. September, 2022, DOI: 10.1007/s11277-022-10037-0.

[8] Z. Wang, X. Dai, and W. Sun, "Tri-beam slot antenna array based on substrate integrated waveguide (SIW) technology," *Int. J. Microw. Wirel. Technol.*, vol. 12, no. 3, pp. 246–251, 2020, DOI: 10.1017/S1759078719001260.

[9] O. M. Haraz, A. Elboushi, S. A. Alshebeili, and A.-R. Sebak, "Dense Dielectric Patch Array Antenna With Improved Radiation Characteristics Using EBG Ground Structure and Dielectric Superstrate for Future 5G Cellular Networks," *IEEE Access*, vol. 2, pp. 909–913, 2014, DOI: 10.1109/ACCESS.2014.2352679.

[10] P. Singh, K. Ray, and S. Rawat, "Design of nature inspired broadband microstrip patch antenna for satellite communication," *Adv. Intell. Syst. Comput.*, vol. 419, pp. 369–379, 2016, DOI: 10.1007/978-3-319-27400-3_33.

[11] P. Singh, K. Ray, and S. Rawat, "Analysis of Sun Flower Shaped Monopole Antenna," *Wirel. Pers. Commun.*, vol. 104, no. 3, pp. 881–894, 2019, DOI: 10.1007/s11277-018-6056-z.

[12] S. Gupta, T. Arora, D. Singh, and K. K. Singh, "Nature inspired golden spiral super-ultra wideband microstrip antenna," *Asia-Pacific Microw. Conf. Proceedings, APMC*, vol. 2018-November, pp. 1603–1605, 2019, DOI: 10.23919/APMC.2018.8617550.

[13] N. Gupta, J. Saxena, and K. S. Bhatia, "Design of Wideband Flower-Shaped Microstrip Patch Antenna for Portable Applications," *Wirel. Pers. Commun.*, vol. 109, no. 1, pp. 17–30, 2019, DOI: 10.1007/s11277-019-06547-z.

[14] W. Mu *et al.*, "A Flower-Shaped Miniaturized UWB-MIMO Antenna with High Isolation," *Electron.*, vol. 11, no. 14, 2022, DOI: 10.3390/electronics11142190.

[15] V. Kathuria, A. Yadav, A. Malik, U. Kumar, and M. R. Tripathy, "Flower shaped antenna for terahertz applications," *IFIP Int. Conf. Wirel. Opt. Commun. Networks, WOCN*, vol. 2016-November, pp. 6–8, 2016, DOI: 10.1109/WOCN.2016.7759886.

[16] U. Keshwala, S. Rawat, and K. Ray, "Design and analysis of eight petal Flower shaped fractal antenna for THz applications," *Optik (Stuttg).*, vol. 241, p. 166942, Apr. 2021, DOI: 10.1016/j.ijleo.2021.166942.

[17] S. Rahman *et al.*, "Nature inspired MIMO antenna system for future mmwave technologies," *Micromachines*, vol. 11, no. 12, pp. 1–11, 2020, DOI: 10.3390/mi11121083.

[18] V. Nath and M. Kumar, "A Compact Flower-Shaped Printed Monopole MIMO Antenna for Wideband Applications," *Radio Sci.*, vol. 54, no. 11, pp. 963–974, 2019, DOI: https://doi.org/10.1029/2019RS006884.

[19] P. Singh, K. Ray, B. H. Ahmad, P. Yupapin, and A. Bandyopadhyay, "A Multiband Tree-shaped Microstrip Antenna for Wireless Communication," vol. 14, no. 4, pp. 17–20, 2022.

[20] J. O. Abolade and D. B. O. Konditi, "Ultra-Compact Slitted Flower-Shaped Dual-Band Monopole Antenna for Modern Portable Devices," *Int. J. Antennas Propag.*, vol. 2022, 2022, DOI: 10.1155/2022/4986861.

[21] I. Ahmad *et al.*, "Maple-leaf shaped broadband optical nano-antenna with hybrid plasmonic feed for nano-photonic applications," *Appl. Sci.*, vol. 11, no. 19, 2021, DOI: 10.3390/app11198893.

[22] U. Keshwala, S. Rawat, and K. Ray, "Nature inspired 21 branches sneezewort/Achillea ptarmica plant growth pattern–shaped antenna for Ku-band applications," *Int. J. RF Microw. Comput. Eng.*, vol. 30, no. 8, p. e22240, 2020, DOI: https://doi.org/10.1002/mmce.22240.

[23] P. Singh, K. Ray, and S. Rawat, "Nature inspired sunflower shaped microstrip antenna for wideband performance," *Int. J. Comput. Inf. Syst. Ind. Manag. Appl.*, vol. 9, no. 2017, pp. 1–8, 2017.

[24] T. Nahar and S. Rawat, "Electromagnetically Coupled Semi-Circular Patch Antenna with Tapered Slotted Ground for V band, W Band and M Band Applications," *Microw. Rev.*, vol. 28, pp. 14–22, Jul. 2022.

[25] S. Singhal, "Compact Wideband Antenna for 60 GHz Millimeter Wave Applications," *Microw. Rev.*, vol. 27, no. 1, pp. 23–27, 2021.

[26] R. Zhou, D. Liu, and H. Xin, "Design of circularly polarized antenna for 60 GHz wireless communications," *Eur. Conf. Antennas Propagation, EuCAP 2009, Proc.*, pp. 3787–3789, 2009.

[27] A. Jaiswal, M. P. Abegaonkar, and S. K. Koul, "Highly Efficient, Wideband Microstrip Patch Antenna with Recessed Ground at 60 GHz," *IEEE Trans. Antennas Propag.*, vol. 67, no. 4, pp. 2280–2288, 2019, DOI: 10.1109/TAP.2019.2894319.

[28] H. Vettikalladi, O. Lafond, and M. Himdi, "High-efficient and high-gain superstrate antenna for 60-GHz indoor communication," *IEEE Antennas Wirel. Propag. Lett.*, vol. 8, pp. 1422–1425, 2009, DOI: 10.1109/LAWP.2010.2040570.

[29] J. G. Kim, H. S. Lee, H. S. Lee, J. B. Yoon, and S. Hong, "60-GHz CPW-fed post-supported patch antenna using micromachining technology," *IEEE Microw. Wirel. Components Lett.*, vol. 15, no. 10, pp. 635–637, 2005, DOI: 10.1109/LMWC.2005.856690.

[30] M. F. Haider, S. Alam, and M. H. Sagor, "V-Shaped Patch Antenna for 60 GHz mmWave Communications," *2018 3rd Int. Conf. Converg. Technol. I2CT 2018*, no. April, pp. 1–4, 2018, DOI: 10.1109/I2CT.2018.8529809.

[31] E. Garcia-Marin, J. L. Masa-Campos, and P. Sanchez-Olivares, "Diffusion Bonding Manufacturing of High Gain W-Band Antennas for 5G Applications," *IEEE Commun. Mag.*, vol. 56, no. 7, pp. 21–27, 2018, DOI: 10.1109/MCOM.2018.1700986.

[32] R. N. Tiwari, P. Kumar, and N. Bisht, "Rectangular microstrip patch antenna with photonic band gap crystal for 60GHz communications," *Prog. Electromagn. Res. Symp.*, pp. 856–859, 2011.

[33] Y. I. A. Al-yasir and R. Abd-alhameed, "Design of Radiation Pattern-Reconfigurable 60-GHz Antenna for 5G Applications," no. December, 2014.

[34] H. yang Xia, J. can Hu, T. Zhang, L. ming Li, and F. chun Zheng, "Integrated 60-GHz miniaturized wideband metasurface antenna in a GIPD process," *Front. Inf. Technol. Electron. Eng.*, vol. 21, no. 1, pp. 174–181, 2020, DOI: 10.1631/FITEE.1900453.